Energy 64 (2014) 734–746

Contents lists available at ScienceDirect

Energy

journal homepage: www.elsevier.com/locate/energy

Optimization mathematical model for the detailed design of air cooled heat exchangers

Juan I. Manassaldi [a,1], Nicolás J. Scenna [a,1], Sergio F. Mussati [a,b,*,1]

[a] CAIMI Centro de Aplicaciones Informáticas. y Modelado en Ingeniería, Universidad Tecnológica Nacional, Facultad Regional Rosario, Argentina
[b] INGAR Instituto de Desarrollo y Diseño (CONICET-UTN), Argentina

ARTICLE INFO

Article history:
Received 30 May 2013
Received in revised form
13 August 2013
Accepted 26 September 2013
Available online 26 October 2013

Keywords:
Air cooled heat exchangers
Optimization
Generalized disjunctive programming
Mathematical programming

ABSTRACT

This paper presents a disjunctive mathematical model for the optimal design of air cooled heat exchangers. The model involves seven discrete decisions which are related to the selection of the type of the finned tube, number of tube rows, number of tube per row, number of passes, fins per unit length, mean fin thickness and the type of the flow regime. Each discrete decision is modeled using disjunctions, boolean variables and logical propositions. The main continuous decisions are: fan diameter, bundle width, tube length, pressure drops and velocities in both sides of the ACHE, heat transfer area, fan power consumption. Then, the resulting generalized disjunctive programming model is reformulated as a mixed integer non-linear programming, implemented in GAMS (general algebraic modeling system) and solved using a branch-and-bound method. The proposed model was successfully verified by comparing the obtained output results with different designs taken from the literature. Then, the model is solved to obtain the optimal designs corresponding to the following optimization criteria: a) minimization the total annual cost which includes investment (heat transfer area) and operating cost (fan power consumption), b) minimization the heat transfer area and c) minimization the fan power consumption. Obtained optimal and sub-optimal designs are compared in detail.

1. Introduction

ACHEs (Air cooled heat exchangers) are widely used to cool process streams with ambient air as the cooling medium rather than water. Environmental concerns such as shortage of make-up water, blow-down disposal and thermal pollution tend to favor the ACHE. Although the capital cost of ACHE is generally high, the operating cost is usually significantly lower than that required by a water-cooled heat exchanger. They are more preferred in arid and/or semi-arid regions and in places where the available water requires extensive treatment to reduce fouling. ACHEs consist of one or more banks of finned tubes (called also tube bundles) over which air is blown by one or more fans. The fans are situated in bays, which are self-contained section of an ACHE. A bay may be made up of multiple tube bundles and may also be served by one or more fans.

Common applications of ACHEs include refineries and petrochemical plants. The following two types of ACHEs widely found in petrochemical plants.

a) The forced draft ACHE is the most economical and most common style air cooler where axial fans used to force air across the fin tube bundle are mounted below the bundle and therefore the mechanical sections are not exposed to the hot exhaust air flow. Also, another advantage of this arrangement is the fact that provides direct access to bundle for replacement.
b) The induced draft ACHE involves axial fans to pull air across the fin tube bundle and it is the second most economical arrangement (Fig. 1). In contrast to the previous arrangement, the fans are positioned above the bundle thus offering greater control of the process fluid and bundle protection due to the additional structure.

Air cooler fans are normally 14–16 ft in diameter. Generally, the design basis is two fan bays. Good-practice design is to keep the ratio of fan diameter area to face area of the tube bundles to 0.4 or above.

The design of ACHEs needs to consider a large number of factors such as heat transfer capacity, pressure drop characteristics,

* Corresponding author. INGAR Instituto de Desarrollo y Diseño (CONICET-UTN), Argentina. Tel.: +54 342 4534451; fax: +54 342 4553439.
E-mail addresses: jmanassaldi@frro.utn.edu.ar (J.I. Manassaldi), nscenna@yahoo.com.ar (N.J. Scenna), mussati@santafe-conicet.gov.ar (S.F. Mussati).
[1] Tel.: +54 341 4480102.

0360-5442/$ – see front matter
http://dx.doi.org/10.1016/j.energy.2013.09.062

Nomenclature

A	heat transfer surface area, m^2
A_{min}	minimum flow area in the tube bank, m^2
A_{face}	face area of the tube bank, m^2
A_{ot}	total outside surface area per unit length, m^2
A_{of}	outside finned area per unit length, m^2
a_0	flow acceleration factor
CRF	capital recovery factor, 1/yr
C_{tb}	cost of heat transfer surface area, $/yr
C_{fan}	cost of fans, $/yr
C_{op}	operating cost, $/yr
C_1, C_2	Boolean variable used to select the type of finned tube (I and II)
c_1, c_2	binary variable used to select the type of finned tube (I and II)
D_r	finned tube root diameter, m
D_i	inside tube diameter, m
D_f	fin outside diameter, m
D_{fan}	fan diameter, m
F_t	LMTD correction factor
F_1, F_2, F_3	Boolean variables used to select the type of flow regime
f_1, f_2, f_3	binary variables used to select the type of flow regime
f_{is}	isothermal friction factor
G_{max}	maximum mass velocity, Kg/(s m^2)
$G_{max,4000}$	maximum mass velocity at Reynolds 4000, kg/(s m^2)
$G_{max,12000}$	maximum mass velocity at Reynolds 12,000, kg/(s m^2)
h_o	heat transfer coefficient, outside surface, W/(m^2 °K)
h_i	tube side heat transfer coefficient, W/(m^2 °K)
h_a	actual outside heat transfer coefficient, W/(m^2 °K)
k_t	thermal conductivity od tube, kW/(m °K)
K_p	tube and layout configuration factor
H_f	fin height, m
L	tube length, m
L_f	mean fin thickness, m
L_1, L_2, L_3	Boolean variables used to select the mean fin thickness
l_1, l_2, l_3	binary variables used to select the mean fin thickness
M	Big-M parameter
N_r	number of tube rows
N_p	number of passes
N_f	fins per unit length, 1/m
N_t	integer variable used to select the number of tube per row
N_3, N_4, N_5, N_6	Boolean variables used to select the number of tube rows
n_3, n_4, n_5, n_6	binary variables used to select the number of tube rows
n_{fan}	number of fans
P_l	longitudinal tube pitch, m
P_t	transverse tube pitch, m
Pr	Prandtl number
P_1, P_2, P_3, P_4, P_5, P_6	Boolean variables used to select the number of tube passes
p_1, p_2, p_3, p_4, p_5, p_6	binary variables used to select the number of tube passes
Q	heat duty, kW
Re	Reynolds number
Re_{eff}	effective Reynolds number
R_{fi}	inside fouling resistance, (°K m^2)/W
R_{fo}	outside fouling resistance, (°K m^2)/W
R_1, R_2, R_3	Boolean variables used to select the range of the *Re* number
r_1, r_2, r_3	binary variables used to select the range of the *Re* number
S_f	fin spacing, m
TAC	total annual cost, $/yr
T_b	bulk temperature, °K
T_w	wall temperature, °K
U_{req}	required overall heat transfer coefficient, W/(°K m^2)
U_D	design overall heat transfer coefficient, W/(°K m^2)
v_{fan}	volumetric flow rate of air, m^3/s
v_{std}	volumetric flow rate of air at standard conditions, m^3/s
v_{oil}	oil velocity in the tube, m/s
W	width of tube bundle, m
W_{motor}	fan power consumption, kW
W_{air}	air mass flow rate, Kg/h
W_{oil}	oil mass flow rate, Kg/h
Greek	
ρ_{air}	air density at bulk temperature, kg/m^3
ρ_{std}	air density at standard condition, kg/m^3
ρ_1	density of the air at the inlet of heat exchanger, kg/m^3
ρ_2	density of the air at the outlet of heat exchanger, kg/m^3
ϕ_p	gas physical property correction factor for pressure drop calculation
ϕ_h	gas physical property correction factor for heat transfer calculation
ΔT_{lm}	logarithmic mean temperature difference for counter-current flow, °K
ΔP_{fan}	pressure drop in the fan, Pa
ΔP_{oil}	pressure drop in the tube-side (oil), kPa
ΔP_{air}	pressure drop in the tube bundle (air), Pa
γ_{rh}	heat transfer row correction factor
γ_{rp}	pressure drop row correction factor
μ_{air}	air viscosity at bulk temperature, Pa s
μ_{oil}	oil viscosity, Pa s
η_{fan}	total fan efficiency
η_{sr}	efficiency of speed reducer
η_{motor}	motor efficiency
Ω_a	actual fin efficiency

physical size and arrangement, required pumping power of process fluid, air flow-rate, types of flow patterns (counter-current flow, co-current flow and cross current flow) among others.

The traditional design procedure of ACHEs is similar to that used for shell and tube heat exchangers. By following design guidelines, the first step of the methodology consists of finding an initial design for the unit using an approximate overall heat transfer coefficient. Then, by using a trial-error the initial design is iteratively modified in order to obtain an acceptable design that satisfy specific tolerance criteria. Although this method can be efficiently used to rate existing units or to obtain new designs via simulation, it is not well suited for optimization especially when many optimization variables should be considered. Certainly, the application of this methodology for a rigorous optimization of ACHEs may be laborious and time consuming if discrete decisions (type of the flow regime, type of the finned tube, number of tube rows, number of tube per row, number of passes, fins per unit length and the mean fin thickness) and operating conditions (velocities, pressure drops, overall transfer coefficient) are considered as optimization variables. For this kind of problem design, the number of possible

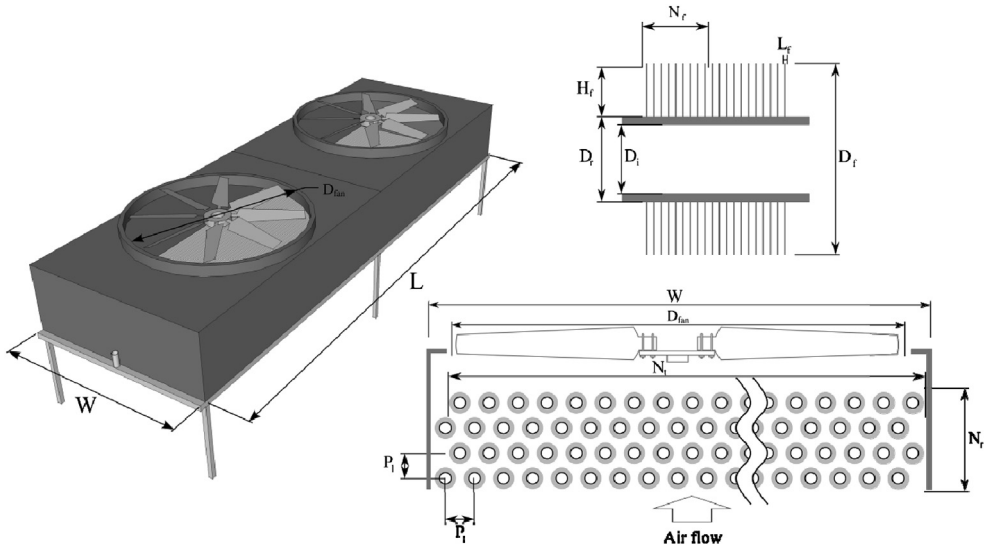

Fig. 1. Typical configuration of an induced-draft air cooled heat exchanger.

combinations to be explored drastically increases as the number of discrete decisions increases.

Several articles dealing with the simulation and optimization of air cooled heat exchangers have been published [1–5].

Doodman et al. 2009 [3] investigated the use of GSA (global sensitivity analysis) and HS (harmony search) algorithm for design optimization of ACHEs from the economic viewpoint. In order to reduce the size of the optimization problem, GSA was performed to examine the effect of the design parameters and to identify the non-influential parameters. Then, HS was applied to optimize influential parameters. For a specific case study, the results obtained by the HS algorithm were compared to those obtained by genetic algorithm (GA). The comparison showed that the HS algorithm predicted better optimal solutions in comparison with GA.

Salimpour and Bahrami 2011 [4] performed a thermodynamic second law analysis in order to investigate the effects of different geometry and flow parameters on the air-cooled heat exchanger performance. For this purpose, the entropy generation due to heat transfer and pressure loss of internal and external flows of the air-cooled heat exchanger was calculated. From the obtained results, it was observed that the total entropy generation has a minimum at special tube-side Reynolds number. Also, it was seen that the increasing of the tube side Reynolds number resulted in an increase of the irreversibility of the air-cooled heat exchanger. The results also showed when air-side Reynolds number decreased, the entropy generation rate of the external flow reduced. Finally, based on the computed results, a new correlation was developed to predict the optimum Reynolds number of the tube-side fluid flow.

Pieve and Salvadori 2011 [5] developed a simplified mathematical model to predict, under various environmental conditions, the performance of an ACSC (air-cooled steam condenser), installed in a waste-to-energy heat recovery plant. For an ACSC, the bottom heat sink is represented by the environmental air, hence the fluctuations of the environmental air temperature undoubtedly affect the performance of the device. Because of the constancy of the temperature on the condensing steam side, the mathematical model is based on the direct application of LMTD (log-mean temperature difference) method. It provides the relation between the air temperature and the volumetric air flow rate, and the main cycle operating parameters. An analysis of the on-site electrical demand has been also performed, which shows that a net benefit is achievable by increasing the air-cooled steam condenser units from six to eight.

For any piece of equipments or processes, the application of mathematical programming techniques allow to simultaneously optimize all the trade-offs existing between alternative arrangements in order to obtain the best design for a given specification design at minimum total cost (investment and operating costs). Some of the models proposed in several application areas which are based on mathematical programming techniques can be found in Vecchietti and Grossmann 1999 [6], van den Heever and Grossmann 1999 [7], Oldenburg and Marquardt 2008 [8], You et al., 2009 [9], Marchetti et al., 2010 [10], Cafaro et al., 2011 [11] Ponce-Ortega et al., 2012 [12], García-Ayala et al., 2012 [13].

This paper presents a disjunctive mathematical programming to optimize both the arrangement and operating conditions of an induced-draft air-cooled heat exchanger (Fig. 1).

2. Problem statement

The optimization problem addresses in this paper may be summarized as follows. Given the flow-rate and inlet/output temperatures of the hydrocarbon (hot stream) to be cooled with air (cold stream), the design problem consists of determining the optimal overall configuration of the ACHE using the following optimization criteria:

a) To minimize the total annual cost including investment (heat transfer area and fans) and operating cost (fan power consumption)
b) To minimize the heat transfer surface area
c) To minimize the fan power consumption.

In the three design problems, all the trade-offs involved by the discrete and continuous decisions are optimized simultaneously. Thus, the selection of the type of the flow regime (laminar, turbulent), the type of the finned tube, number of tube rows, number of tube per row, number of passes, fins per unit length and the mean fin thickness, velocities and pressure drops in both sides of ACHE are obtained as a result of the model.

3. Mathematical model and assumptions

In this section, the assumptions and the mathematical model for the ACHE shown in Fig. 1 are presented.

3.1. Assumptions

The following are some of the main assumptions used to derive the mathematical model.

- Average physicochemical properties for the hydrocarbon and air are assumed.
- Mass flow-rate, inlet and outlet temperatures of both hot and cold streams, fouling factor and maximum allowable pressure drops in each side of the equipment are model parameters (given and known values).
- Tubes having a 1 inch diameter arranged on triangular pitch are considered.
- The hydrocarbon flows in the inner tube while the air flows in the outer tube.
- Two fan bays with one tube bundle are assumed.

3.2. Detailed mathematical model

By adopting the above assumptions, the following mathematical model was derived. Detailed correlations considered in the model were used and they were chosen based on the suggestions found in several books of heat transfer equipments [14–16]. They are valid in the range of variables covered in this study. The nomenclature of the main optimization variables is included in Fig. 1.

3.2.1. Design equation

3.2.1.1. Heat transfer area. The heat transfer area (A) is computed as follows:

$$Q = U_{req} A F_t \Delta T_{1m} \tag{1}$$

where U_{req} refers to the required overall heat transfer coefficient and ΔT_{lm} is the LMTD (log mean temperature difference) which is corrected by the factor (F_t). As will be described later, the factor F_t depends on the number of passes (N_p) and number of rows (N_r) which in turn determine the type of flow regime.

The following constraint relates the heat transfer area with the number of rows (N_r), the number of tubes per row (N_t), the total outside surface area per unit length (A_{ot}) and the tube length (L):

$$A = N_r N_t L A_{ot} \tag{2}$$

N_r and N_t are defined as integer variables. A_{ot} refers to the total outside surface area per unit length. According to eq. (3), A_{ot} depends on the following optimization variables: finned tube root diameter (D_r), mean fin thickness (L_f), fins per unit length (N_f), and fin outside diameter (D_f) and it is computed as follows:

$$A_{ot} = \pi D_r \left(1 - L_f N_f\right) + A_{of} \tag{3}$$

where A_{of} is the outside finned area per unit length and it is computed as follows:

$$A_{of} = 2N_f \frac{\pi}{4}\left(D_f^2 - D_r^2\right) + \pi D_f L_f N_f \tag{4}$$

where D_r refers to the outside diameter of bare tube and it is considered as a model parameter (given and known value). The fin outside diameter (D_f) depends on the fin height (H_f) and D_r, as indicated in eq. (5)

$$D_f = D_r + 2H_f \tag{5}$$

A_{ot} is also used in eq. (8) to compute the design overall heat transfer coefficient [U_D].

The minimum flow area in the tube bank (A_{min}) and the face area of the tube bank (A_{face}) are given by eqs. (6), (7). They are used in eq. (21) to compute the flow acceleration factor (a_0) which in turn is used in eq. (16) to compute the pressure drop (ΔP_{air}).

$$A_{min} = N_t L\left(P_t - D_r - 2N_f H_f L_f\right) \tag{6}$$

$$A_{face} = WL \tag{7}$$

where P_t and W refer, respectively, to the transverse tube pitch and width of tube bundle.

As it will also be described later in Section 3.2.2, the optimal values of the fins per unit length (N_f), the fin height (H_f) and the transverse tube pitch (P_t) are selected from disjunction D1 while the value of the mean fin thickness (L_f) is selected from disjunction D2.

The design overall (U_D) heat transfer coefficient is computed as follows:

$$U_D = \left[\left(\frac{1}{h_i} + R_{fi}\right)\left(\frac{A_{ot}}{\pi D_i}\right) + \left(\frac{A_{ot}\ln\left(D_r/D_i\right)}{2\pi k_t}\right) + \left(\frac{1}{h_a} + R_{fo}\right)\right]^{-1} \tag{8}$$

$$h_a = h_o\left[1 - (1 - \Omega_a)\left(\frac{A_{of}}{A_{ot}}\right)\right] \tag{9}$$

where h_i, h_0 and h_a are the local heat transfer coefficients. On the other hand, R_{fi}, R_{fo} and k_t are model parameters (fixed values) and they refer, respectively, to the inside and outside fouling resistances and the thermal conductivity whereas Ω_a refers to the fin efficiency (model variable). The variable h_i is given by eq. (10).

$$h_i = c_1\left(\frac{k_i}{D_i}\right) Re_i^{c_2} Pr_i^{c_3} \quad \text{with} \quad Re_i = \frac{4W_{oil}N_p}{\pi D_i N_t N_r \mu_{oil}} \tag{10}$$

where c_1, c_2 and c_3 are numerical constants and they can be found in elsewhere [14–16]. The parameters W_{oil} and μ_i refer, respectively, to the oil flow-rate and viscosity whereas D_i is the inner diameter of the tube. As will be described in Section 3.2.4 the correlation used to compute h_0 is selected from three options depending on the Reynolds number.

In order to guarantee a feasible design, the following inequality constraint is imposed:

$$U_D \geq U_{req} \tag{11}$$

3.2.1.2. Fan and motor sizing. The fan power consumption [W_{motor}] is expressed as:

$$W_{motor} = \frac{\Delta P_{fan} \nu_{fan}}{\eta_{fan}\eta_{sr}\eta_{motor}} \tag{12}$$

where ΔP_{fan} and ν_{fan} refer, respectively, to the total pressure drop in the fan and volumetric flow rate of air through fan. η_{fan}, η_{sr} and η_{motor} are the efficiencies of the fans, speed reducer and motor, respectively. The total pressure drop in the fan is computed as follows:

$$\Delta P_{fan} = \Delta P_{air} + \left(\frac{1+0.13}{2}\right)\rho_2 \left(\frac{\frac{W_{air}}{n_{fan}\rho_2}}{\pi\left(D_{fan}\right)^2}\right)^2 \quad (13)$$

where n_{fan} is the number of fans and D_{fan} and W_{air} refer to the diameter of fans and mass flow-rate of air, respectively.

The following constraints are used to ensure that the area required by the fans is at least 40 percent of the bundle face area and that the fan diameter must be 6 inches less than the bundle width.

$$n_{fan}\frac{\pi}{4}\left(D_{fan}\right)^2 \geq 0.4(W \times L) \quad (14)$$

$$D_{fan} \leq W - 0.1524\ \text{m} \quad (15)$$

3.2.1.3. Pressure drops. The model considers the pressure drop in air and oil sides. The pressure drop in the air-side (ΔP_{air}) is given by:

$$\Delta P_{air} = \frac{4G_{max}^2 N_r}{2\rho_{air}}\left(f_{is}\gamma_{rp}\phi_p + a_0\right) \quad (16)$$

where f_{is}, γ_{rp} and ϕ_p are, respectively, the isothermal friction factor, pressure drop row correction factor and gas physical property correction factor. The factors f_{is} and ϕ_p are computed by eqs. (17), (20) whereas γ_{rp} is selected from the disjunction D4, as will be described in Section 3.2.5.

$$f_{is} = K_p\left(0.08 + \frac{38.2}{Re_{eff}} + 0.15\left(Re_{eff}\right)^{-0.21}\right) \quad (17)$$

where K_p and Re_{eff} refer to the tube and layout configuration factor and the effective Reynolds number and they are computed by eqs. (18), (19), respectively. Finally, in eq. (16), the variable a_0 refers to the flow acceleration factor and depends on A_{min}/A_{face}, N_r and density of air (ρ_{air}, ρ_1, ρ_2) as indicated in eq. (21).

$$K_p = \left(0.9 + \frac{1.6}{1+\frac{(P_t-D_f)}{D_r}}\right)e^{-0.5\left(\frac{(P_t-D_f)}{D_r}\right)^n} \quad (18)$$

$$Re_{eff} = Re\left(\frac{1}{S_f}\right)^{-3\exp\left(-0.0258\left(\frac{S_f}{H_f}\right)^2\sqrt{Re}\right)\left(\frac{D_f}{D_r}\right)^{(-1.4)}} \quad (19)$$

where S_f refers to the fin spacing

$$\phi_p = \left(\frac{T_w}{T_b}\right)^{0.3} \quad (20)$$

$$a_0 = \left(\frac{1+\left(\frac{A_{min}}{A_{face}}\right)^2}{4N_r}\right)\rho_{air}\left(\frac{1}{\rho_2}-\frac{1}{\rho_1}\right) \quad (21)$$

ρ_1 and ρ_2 refer to inlet and outlet densities and ρ_{air} is the average density.

3.2.1.4. Cost model. The TAC (total annual cost) is used as objective function and is computed as follows:

$$TAC = CRF\, C_{tb} + CRF\, n_{fan} C_{fan} + n_{fan} C_{op} \quad (22)$$

where CRF (capital recovery factor) and n_{fan} refer to the capital recovery factor and number of fans.

$$CRF = \frac{(i)(1+i)^y}{(1+i)^y - 1} \quad (23)$$

where y and i are the projected lifetime of ACHE (5 years) and the annual interest rate, expressed as a fraction (0.05). C_{tb} and C_{fan} are, respectively, the costs of the heat transfer area and fans and C_{op} refers to the operating cost. Each cost-item is taken from Ref. [17] and computed according to the following constraints:

$$C_{tb}\ [\$/\text{yr}] = K_1 10^{3.6418+0.40538\ \log_{10}(A)} \quad (24)$$

where K_1 is given by:

$$K_1 = 1.53 + 1.2710^{-0.06154+0.0473\ \log_{10}(3.44)} \quad (25)$$

$$C_{fan}[\$/\text{yr}] = K_2 2.2\left(1 + 0.2164\log\left(\Delta P_{fan}\right)\right) \quad (26)$$

where K_2 depends on the volumetric standard flow rate per fan (v_{std}) and is given by eq. (27). ΔP_{fan} refers to the total pressure difference across the fan and is computed by eq. (13):

$$K_2 = 10^{2.9471+0.3302\log_{10}(v_{std})+0.1969\ \log_{10}(v_{std})^2} \quad (27)$$

$$C_{op}[\$/\text{yr}] = 0.06\ 8000\ W_{motor} \quad (28)$$

As mentioned earlier, a disjunctive programming model (GDP (generalized disjunctive programming)) is first developed. Each discrete decision is modeled through Boolean variables and disjunctions. Also, logic propositions are used to model relationships that exist between discrete decisions. Then, the proposed model is reformulated as a MINLP (mixed integer non linear programming) model. Next, each disjunction and logic propositions including the corresponding reformulations are presented in detail.

3.2.2. Selection of the type of finned tube

The mathematical model embeds two types of finned tube and the final selection of one of them involves the following disjunction.

$$\begin{bmatrix} C_1 \\ H_f = 12.7 \\ N_f = 354.33 \\ P_t = 57.15 \end{bmatrix} \vee \begin{bmatrix} C_2 \\ H_f = 15.875 \\ N_f = 393.7 \\ P_t = 63.5 \end{bmatrix} \quad (D1)$$

where C_1 and C_2 are Boolean variables corresponding to the type of finned tube I and II, respectively. As shown, if option C_1 is selected (C_1 = True) then the corresponding values of the fin height (H_f), fins per unit length (N_f) and transverse tube pitch (P_t) should be 12.7 mm, 354.33 (1/m) and 57.15 mm, respectively. Disjunctive D1 is then transformed into four equality constraints [eqs. (29)–(32)] whereas Boolean variables C_1 and C_2 are transformed into integer variables c_1 and c_2, respectively. At this point it should be observed the difference between C_1 (boolean variable: true or false) and c_1 (binary variable: 1 or 0); in other words, if C_1 = True, then $c_1 = 1$.

$$H_f = 12.7\, c_1 + 15.875\, c_2 \quad (29)$$

$$N_f = 354.33\, c_1 + 393.7\, c_2 \quad (30)$$

$$P_t = 57.15\, c_1 + 63.5\, c_2 \tag{31}$$

The following constraint ensures that only one type of finned tube is selected.

$$c_1 + c_2 = 1 \tag{32}$$

3.2.3. Selection of the mean fin thickness (L_F)

The following disjunction (D2) is imposed in order to select one from three options for the width of ACHE (0.305, 0.330 and 0.356 mm).

$$\begin{bmatrix} L_1 \\ L_F = 0.305 \end{bmatrix} \vee \begin{bmatrix} L_2 \\ L_F = 0.330 \end{bmatrix} \vee \begin{bmatrix} L_3 \\ L_F = 0.356 \end{bmatrix} \tag{D2}$$

The Boolean variables L_1, L_2 and L_3 in disjunctive D2 are then transformed into integer variables l_1, l_2 and l_3, respectively, as indicated from eqs. (33) to eq. (34).

$$L_F = l_1 0.305 + l_2 0.330 + l_3 0.356 \tag{33}$$

In order to select only one option, the following constraint should be satisfied.

$$l_1 + l_2 + l_3 = 1 \tag{34}$$

3.2.4. Selection of the flow regimen (Re) and heat transfer coefficient (h_0) for the air stream

As known, the correlation used to compute the local heat transfer coefficient depends on the flow regimen. The model embeds three types of flow regimes and each one of them is related to the Boolean variables R_1, R_2, and R_3.

$$\begin{bmatrix} R_1 \\ Re \le 4000 \\ h_o = h_{Re\le 4000} \end{bmatrix} \vee \begin{bmatrix} R_2 \\ 4000 \le Re \le 12000 \\ h_o = h_{4000\le Re\le 12000} \end{bmatrix} \vee \begin{bmatrix} R_3 \\ Re \ge 12000 \\ h_o = h_{Re\ge 12000} \end{bmatrix} \tag{D3}$$

Then, each term in D3 is modeled using the big-M formulation [eqs. (35)–(38), eqs. (42)–(45) and eqs. (46)–(52)]. If the optimal Reynolds number is lower than 4000, then the Boolean variable R_1 is True in disjunction D3 and its corresponding binary variable r_1 in eqs. (35)–(37) is 1. Certainly, for $r_1 = 1$ [$r_2 = r_3 = 0$ by eq. (53)], the constraint (35) ensures that the Re number will be lower than 4000 and the constraints (36) and (37) ensure that the appropriate correlation $h_{Re\le 4000}$ given by eq. (38) will be used to compute h_0. From eqs. (36), (37) it can be clearly observed that for $r_1 = 1$ then $h_0 = h_{Re\le 4000}$ without violating eqs. (43), (44), (48) and (49). As will be described later, a similar reasoning can be made for $r_2 = 1$ ($r_1 = r_3 = 0$) and $r_3 = 1$ ($r_1 = r_2 = 0$).

$$Re \le 4000 + M(1 - r_1) \tag{35}$$

$$h_o \le h_{Re\le 4000} + M(1 - r_1) \tag{36}$$

$$h_o \ge h_{Re\le 4000} - M(1 - r_1) \tag{37}$$

where M refers to the big-M factor. The numerical value for M is suggested to be 4–5 times greater than the maximum value that may be obtained. In eq. (35), $M = 20{,}000$ whereas in eqs. (36) and (37) $M = 100$.

$$h_{Re\le 4000} = 0.4 Re^{-0.383} \left(\frac{A_{ot}}{A_r}\right)^{-0.15} \gamma_{rh} \phi_h C_p G_{max} Pr^{-2/3} \tag{38}$$

In eqs. (38), (45), (51) and (52), γ_{rh} refers to the heat transfer row correction factor and is selected from the disjunction D4 and ϕ_h is the gas physical property correction factor and is computed as follows:

$$\phi_h = \left(\frac{T_w}{T_b}\right)^{0.4} \tag{39}$$

where T_w and T_b refer to the wall and bulk temperatures. G_{max} is the maximum air mass velocity which is given by eq. (40).

$$G_{max} = \frac{W_{air}}{A_{min}} \tag{40}$$

The dependence of the Reynolds number on the inner diameter (D_r) and G_{max} is given by eq. (41). It should also be mentioned that the Reynolds number (type of flow-regime) affects the correction factor for the LMTD, as will be described later in Section 3.2.8.

$$Re = \frac{G_{max} D_r}{\mu_{air}} \tag{41}$$

Based on a similar reasoning previously applied for $Re \le 4000$, the following constraints are derived for $Re \ge 12{,}000$ [from eqs. (42)–(45)] and for $4000 \le Re \le 12{,}000$ [from eqs. (46) and (52)].

$$Re \ge 12\,000 - M(1 - r_3) \tag{42}$$

$$h_o \le h_{Re\ge 12000} + M(1 - r_3) \tag{43}$$

$$h_o \ge h_{Re\ge 12000} - M(1 - r_3) \tag{44}$$

$$h_{Re\ge 12\,000} = 0.4\, Re^{-0.4} \left(\frac{A_{ot}}{A_r}\right)^{-0.15} \gamma_{rh} \phi_h C_p G_{max} Pr^{-2/3} \tag{45}$$

$$Re \le 12\,000 + M(1 - r_2) \tag{46}$$

$$Re \ge 4000 - M(1 - r_2) \tag{47}$$

$$h_o \le h_{4000\le Re\le 12\,000} + M(1 - r_2) \tag{48}$$

$$h_o \ge h_{4000\le Re\le 12\,000} - M(1 - r_2) \tag{49}$$

$$h_{4000\le Re\le 12\,000} = (h_{Re=4000} - h_{Re=12\,000}) \left(\frac{12\,000 - Re}{8000}\right) + h_{Re=12\,000} \tag{50}$$

where:

$$h_{Re=4000} = 0.4\, Re^{-0.383} \left(\frac{A_{ot}}{A_r}\right)^{-0.15} \gamma_{rh} \varphi_h C_p G_{max,4000} Pr^{-2/3} \tag{51}$$

$$h_{Re=12000} = 0.4\, Re^{-0.383} \left(\frac{A_{ot}}{A_r}\right)^{-0.15} \gamma_{rh} \varphi_h C_p G_{max,12\,000} Pr^{-2/3} \tag{52}$$

In eqs. (42), (46) and (47) the value of M was set at 20,000 whereas in eqs. (43), (44), (48) and (49) M was set at 100.

Finally, the following constraint ensures the selection of only one type of flow regime.

$$r_1 + r_2 + r_3 = 1 \tag{53}$$

3.2.5. Selection of the number of tube rows and the corresponding heat transfer and pressure drop row correction factors

According to the specific literature on air cooled design [14,18], the tubes are preferred to be arranged in shallow rectangular bundles with the number of tube rows (N_r) usually between 3 and 6. A small number of tube rows are used in order to keep the air-side pressure drop low.

As mentioned earlier, the heat transfer and pressure drop row correction factors (γ_{rh}) and (γ_{rp}) used in eqs. (16), (38), (45), (51) and (52) depend on the number of tube rows. Repeating a similar reasoning as in the previous selection, the following disjunctions and inequality constraints are proposed to consider the relationship between N_r, γ_{rh} and γ_{rp}.

$$\begin{bmatrix} N_3 \\ N_r = 3 \\ \gamma_{rh} = f\left(N_r, P_l/D_f\right) \\ \gamma_{rp} = f\left(N_r, P_l/D_f, Re\right) \end{bmatrix} \vee \begin{bmatrix} N_4 \\ N_r = 4 \\ \gamma_{rh} = 1 \\ \gamma_{rp} = 1 \end{bmatrix} \vee \begin{bmatrix} N_5 \\ N_r = 5 \\ \gamma_{rh} = 1 \\ \gamma_{rp} = 1 \end{bmatrix} \vee \begin{bmatrix} N_6 \\ N_r = 6 \\ \gamma_{rh} = 1 \\ \gamma_{rp} = 1 \end{bmatrix} \tag{D4}$$

$$N_r = n_3 3 + n_4 4 + n_5 5 + n_6 6 \tag{54}$$

$$n_3 + n_4 + n_5 + n_6 = 1 \tag{55}$$

As shown, if N_3 is True in D4, then, $N_r = 3$ and therefore, from eqs. (54) and (55), $n_3 = 1$ ($n_4 = n_5 = n_6 = 0$) and the second terms in eqs. (56) and (57) are not considered which ensures that the factor γ_{rh} is computed using the appropriate correlation [$\gamma_{rh} = f(N_r, P_l/D_f)$] without violating eqs. (58)–(63). From eqs. (58) to (63), it can be clearly seen that if $n_4 = 1$ or $n_5 = 1$ or $n_6 = 1$, then $\gamma_{rh} = 1$.

$$\gamma_{rh} \le f\left(N_r, P_l/D_f\right) + M(1 - n_3) \tag{56}$$

$$\gamma_{rh} \ge f\left(N_r, P_l/D_f\right) - M(1 - n_3) \tag{57}$$

$$\gamma_{rh} \le 1 + M(1 - n_4) \tag{58}$$

$$\gamma_{rh} \ge 1 - M(1 - n_4) \tag{59}$$

$$\gamma_{rh} \le 1 + M(1 - n_5) \tag{60}$$

$$\gamma_{rh} \ge 1 - M(1 - n_5) \tag{61}$$

$$\gamma_{rh} \le 1 + M(1 - n_6) \tag{62}$$

$$\gamma_{rh} \ge 1 - M(1 - n_6) \tag{63}$$

The value assumed for M from eq. (56) and (63) was 10.

Similar inequality constraints are also proposed to compute the value of γ_{rp}.

3.2.6. Selection of the number of passes (N_p)

In typical designs of ACHE, the number of pass (N_p) varies from 1 to 6. Then, this suggestion is introduced by the following disjunction and constraints.

$$\begin{bmatrix} P_1 \\ N_p = 1 \end{bmatrix} \vee \begin{bmatrix} P_2 \\ N_p = 2 \end{bmatrix} \vee \begin{bmatrix} P_3 \\ N_p = 3 \end{bmatrix} \vee \begin{bmatrix} P_4 \\ N_p = 4 \end{bmatrix} \vee \begin{bmatrix} P_5 \\ N_p = 5 \end{bmatrix} \vee \begin{bmatrix} P_6 \\ N_p = 6 \end{bmatrix} \tag{D5}$$

$$N_p = p_1 + p_2 2 + p_3 3 + p_4 4 + p_5 5 + p_6 6 \tag{64}$$

$$p_1 + p_2 + p_3 + p_4 + p_5 + p_6 = 1 \tag{65}$$

In addition, the number of passes (N_p) strongly depends on the number of tube rows (N_r) and flow geometry. This dependence is imposed in the model by logic propositions (L1–L11), as it will be shown in the Section 3.2.8.

3.2.7. Selection of the number of tubes per row (N_t)

The optimization variable N_t refers to the number of tubes per row and is directly defined as an integer variable.

3.2.8. Selection of the correction factor F_t in terms of number of tube passes and number of tube rows

As mentioned in eq. (1), the factor F_t corrects the LMTD (log mean temperature difference) for any deviation from true counter-current flow. In air cooled heat exchanger, the factor F_t depends on flow geometry, precisely on the number of tube rows N_r, the number of tube passes N_p and whether the tube-side fluid is mixed in a header or unmixed in U-tubes. In ACHEs, the air flows substantially unmixed upward across the bundles and the process fluid can flow back and forth and downward as directed by the pass arrangement. In this paper, the value of F_t is selected from three potential values based on several heat exchanger arrangements involving multiple tubes, several shells passes and cross-flow, as described below (Serth 2007 [14]).

1) For one tube pass, the flow pattern approaches the unmixed–unmixed cross flow. Because the inlet and outlet temperatures of the hot and cold streams are assumed as given, then the value of F_t should be 0.9 ($f_1 = 1$).
2) For two tube passes, a different flow pattern from the previous case is obtained. The tube-side fluid is mixed in a return header between passes and the value of F_t should be 0.967 ($f_2 = 1$).
3) For three tube passes, the flow pattern depends on N_r. Then, there are two possibilities in terms of the number of tube rows (N_r): 3 or 6. For $N_r = 3$, the flow pattern approaches the true counter-flow and then F_t should be 1 ($f_3 = 1$). For $N_r = 6$, mixing of the tube-side fluid between passes is obtained as in case 2) and then F_t should also be 0.967 ($f_2 = 1$).
4) For four or more tube passes, the flow pattern approaches the true counter-flow and the value of F_t should be 1 ($f_3 = 1$).

Thus, three options for the correction factor (F_t) are possible. Then, each option is related to a Boolean variable (F_1, F_2 and F_3) through disjunction D6. Also, the logic propositions L1– L7 with their corresponding inequality constraints [eqs. (66)–(74)] are used to select the value of F_t in terms of the number of tube passes and the number of tube rows.

$$\begin{bmatrix} F_1 \\ F_t = 0.9 \end{bmatrix} \vee \begin{bmatrix} F_2 \\ F_t = 0.967 \end{bmatrix} \vee \begin{bmatrix} F_3 \\ F_t = 1 \end{bmatrix} \tag{D6}$$

$$F_t = 0.9 f_1 + 0.967 f_2 + 1 f_3 \tag{66}$$

The selection of only one correction factor is imposed by eq. (67).

$$f_1 + f_2 + f_3 = 1 \tag{67}$$

$$P_1 \Rightarrow F_1 \tag{L1}$$

$$1 - p_1 + f_1 \geq 1 \tag{68}$$

As shown in eq. (68), if only one tube pass is selected, $p_1 = 1$ [$p_2 = p_3 = p_4 = p_5 = p_6 = 0$ from eq. (65)] then $f_1 = 1$ [$f_2 = f_3 = 0$ from eq. (67)] and therefore, from eq. (66), $F_t = 0.9$.

As mentioned earlier, for two tube passes, the tube-side fluid is mixed in a return header between passes and the following disjunction and constraint are used to select the appropriate factor ($F_t = 0.967$; $f_2 = 1$).

$$P_2 \Rightarrow F_2 \tag{L2}$$

$$1 - p_2 + f_2 \geq 1 \tag{69}$$

For three tube passes, the following options are possible:

a) For $N_p = 3$ and $N_r = 3$, the flow pattern approaches the true counter-flow and the value of F_t should be 1 ($f_3 = 1$). Therefore, eq. (70) must be satisfied:

$$P_3 \wedge N_3 \Rightarrow F_3 \tag{L3}$$

$$1 - p_3 + 1 - N_3 + f_3 \geq 1 \tag{70}$$

b) For $N_p = 3$ and $N_r = 6$, and the flow pattern is similar to that described for two tube passes. Then, for this flow geometry ($N_p = 3$, $N_r = 6$), eq. (71) should be satisfied.

$$P_3 \wedge N_6 \Rightarrow F_2 \tag{L4}$$

$$1 - p_3 + 1 - N_6 + f_2 \geq 1 \tag{71}$$

Finally, the following constraints [eqs. (72)–(74)] apply for $N_r \geq 4$ where the flow pattern approaches the true counter-flow and the appropriate correction value is selected when $f_3 = 1$.

$$P_4 \Rightarrow F_3 \tag{L5}$$

$$P_5 \Rightarrow F_3 \tag{L6}$$

$$P_6 \Rightarrow F_3 \tag{L7}$$

$$1 - p_4 + f_3 \geq 1 \tag{72}$$

$$1 - p_5 + f_3 \geq 1 \tag{73}$$

$$1 - p_6 + f_3 \geq 1 \tag{74}$$

3.2.9. Logic propositions relating the number of passes and the number of rows

Different options are possible between the number of passes and the number of rows which lead to different arrangements. Certainly, depending on the number of rows (N_r), there may be more than one option for the number of passes (N_p). For instance, Figs. 2 and 3 illustrate the possible alternatives when $N_r = 3$ and $N_r = 6$.

As shown in Fig. 2, when $N_r = 3$, the number of passes may be 1 (Fig. 2a) or Fig. 3 (Fig. 2b). Similar arrangements are obtained for $N_r = 5$. On the other hand, as shown in Fig. 3, the number of alternatives increases when $N_r = 6$ compared to when $N_r = 3$. Certainly, if $N_r = 6$, the optimal number of passes can be 1, 2, 3 or 6 as shown respectively in Fig. 3a, b, c or d.

In order to embed all possible options for each number of passes, the number of passes should be a divisor of the number of tube rows. Each disjunction proposed for each number of tube rows and its corresponding equations are presented next.

For $N_r = 3$:

$$N_3 \Rightarrow P_1 \vee P_3 \tag{L8}$$

$$1 - n_3 + p_1 + p_3 \geq 1 \tag{75}$$

As mentioned in previous sections, N and P and n and p refer, respectively, to the Boolean and binary variables corresponding to the selection of the number of row and the number of passes.

According to eqs. (75) and eq. (67), if N_3 = True and consequently $n_3 = 1$, then $p_1 = 1$ or $p_3 = 1$ [eq. (65) avoid the possibility that p_1 and p_3 can be 1].

For $N_r = 4$:

$$N_4 \Rightarrow P_1 \vee P_2 \vee P_4 \tag{L9}$$

$$1 - n_4 + p_1 + p_2 + p_4 \geq 1 \tag{76}$$

For $N_r = 5$:

$$N_5 \Rightarrow P_1 \vee P_5 \tag{L10}$$

$$1 - n_5 + p_1 + p_5 \geq 1 \tag{77}$$

For $N_r = 6$:

$$N_6 \Rightarrow P_1 \vee P_2 \vee P_3 \vee P_6 \tag{L11}$$

$$1 - n_6 + p_1 + p_2 + p_3 + p_6 \geq 1 \tag{78}$$

3.2.10. Objective function

As mentioned in the problem statement, the model will be solved for three optimization criteria defined by the following objective functions and the obtained solutions will be analyzed and compared in detail.

OF_1: To minimize the heat transfer area (A)
OF_2: To minimize the fan power consumption (W_{Motor})
OF_3: To minimize the TAC (total annual cost)

The optimization mathematical model involves 155 variables (21 integer variables) and 168 constraints. It is combinatory and non-linear and is implemented in GAMS (general algebraic modeling system). SBB (Standard Branch and Bound) is used as solver for the resulting MINLP model (Brooke 1992 [19]). It is based on a combination of the Standard Branch and Bound method known from Mixed Integer Linear Programming and some of the standard NLP (non-linear programming) solvers already supported by GAMS.

4. Applications of the developed MINLP model. Discussion of results

In this section, the verification of the proposed model and optimization results are presented through three case studies. The

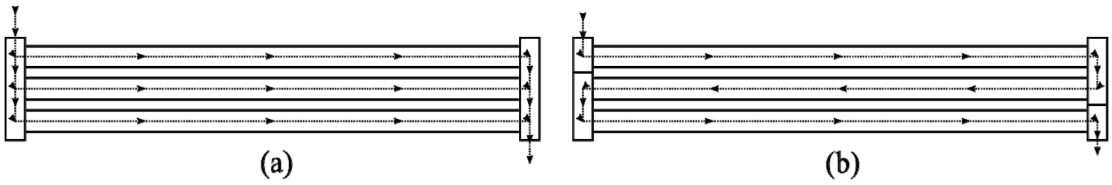

Fig. 2. Alternative options of configuration for $N_r = 3$.

parameter data set listed in Table 1 was assumed for all examples. All examples are solved using a 3.3 GHz AMD Six-Core processor and 4 GB RAM.

4.1. Case study I. Verification of the proposed model

This case study deals with the verification of the model. In order to verify the accuracy of the proposed model, obtained output results are compared with data taken from the literature.

A rigorous model validation should be conducted jointly with heater manufacturers and/or petrochemical industries because numerous and complete data set of real designs can be provided by them. Moreover, this data set could be efficiently used to adjust the model parameters in order to improve the accuracy of the model if this is necessary. Because of real and detailed designs provided by manufacturers are not available in the open literature to validate the proposed model, designs data taken from Serth 2007 [14] are considered for comparison purposes since the majority of the variables are provided. However, it should be mentioned that an iterative solution procedure based on simulation runs has been applied in Serth 2007 [14] instead of optimization techniques. Consequently, the values reported in Ref. [14] and used for comparison are not optimal. For recreating the case study for verification purpose, several optimization variables in the proposed MINLP model are fixed at the same values as in Serth 2007 [14]. Precisely, the variables that were fixed including the numerical values are listed in Table 2. Thus, in this case study the proposed mathematical model is used as a "simulator" in contrast to case study II where it is used as an optimizer.

In addition, solution predicted by XACE (air coolers and economizers) is also used for comparison. XACE is a specific software which uses HTRI's (Heat Transfer Research, Inc.) latest point-wise methods and is widely used to design, rate and simulate the performance of air coolers and economizers. XACE provides multiple options for process and geometry specifications that must be defined by users as input data. In contrast to this, one of the major benefits of the proposed mathematical model is that it allows to optimize the configuration and the dimensions of the equipment.

In Table 3, the resulting values for the main process variables are reported. The solution obtained from the model by simulation is hereafter referred as Design_1 (forth column of Table 3).

As is shown in Table 3, the obtained values for Design_1 are in agreement with the design reported in Serth 2007 [14] and the result predicted by XACE simulator. It should be mentioned that the values reported by Serth 2007 [14] for the air/oil side pressure drops and tube side heat transfer coefficient differ from the values predicted by XACE simulator and GDP model because of the correlations used for calculation. For instance, in Serth 2007 [14], the flow acceleration factor (a_0), the isothermal friction factor (f_{is}), the pressure drop row correction factor (γ_{rp}) and the gas physical property correction factor (ϕ_p) are not considered. However, the differences are not significant.

4.2. Case study II. Optimization results

In this section, the proposed mathematical model was solved by considering three different objective functions and by "relaxing" the variable values that were fixed in Table 2 in Case Study I (model verification). They are now considered as decision variables. Precisely, the model was solved for each objective function presented

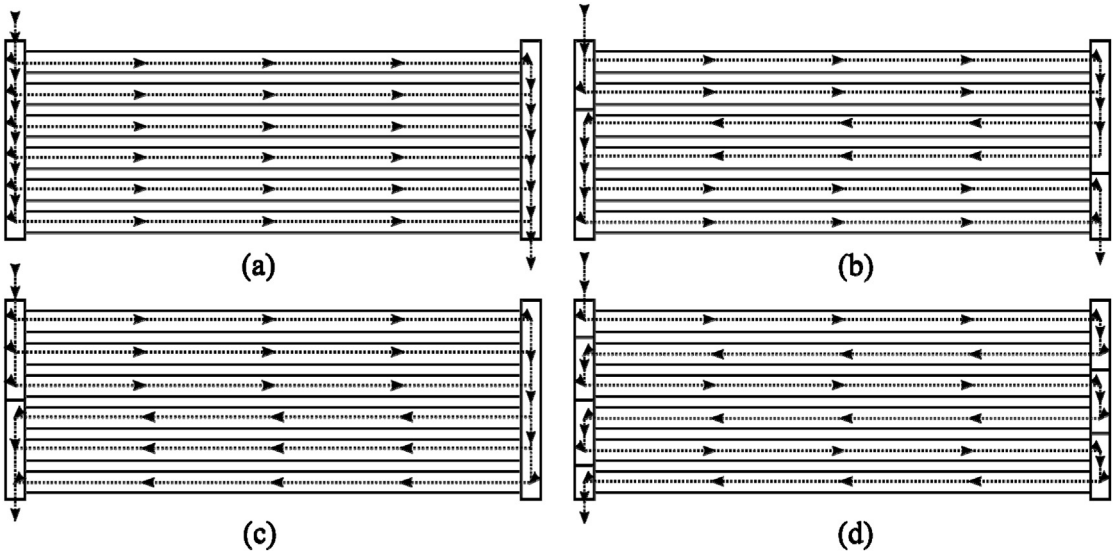

Fig. 3. Alternative options of configuration for $N_r = 6$.

Table 1
Values of model parameters used in all case studies.

Process		
Air temperature in/out	[°K]	308.2/338.8
Oil temperature in/out	[°K]	394.3/338.8
Flow rate oil	[kg/s]	31.5
Tube OD	[mm]	25.4
Tube ID	[mm]	20.574

earlier (OF_1, OF_2 and OF_3) and the obtained optimal results are compared in Table 4.

As expected, the obtained results indicate that the optimal air cooler's design depends strongly on the objective function used for optimization. For instance, the highest value of fan power consumption was obtained when the heat transfer area (OF_1) was minimized and vice versa, the highest value of the heat transfer area was obtained when the fan power consumption (OF_2) was minimized.

From the results listed in Table 4 it can be clearly observed that the tube length and bundle width obtained for OF_1 are much shorter than for OF_2 and OF_3. Certainly, reductions of about 3 and 1 m are reached for the tube length and bundle width compared to OF_2 and OF_3. In addition, the fan diameter and the heat transfer area for OF_1 are also shorter than that obtained for OF_2 and OF_3. However, the air side and oil side pressure drops for OF_1 are significantly greater than those obtained for OF_2 and OF_3. These results can be explained by the increase of the velocities of both fluids in order to improve the heat transfer coefficients resulting in higher pressure drops.

The obtained results also reveal that the optimal fins geometry obtained for both OF_1 and OF_3 ($N_f = 354.33$, $H_f = 12.7$ mm and $L_f = 0.36$ mm) are the same but with a different arrangement compared to OF_2 ($N_f = 393.7$, $H_f = 15.875$ mm and $L_f = 0.3$ mm). For the designs OF_2 and OF_3, the optimal number of passes (N_p) is 3 and the number of tubes per rows (N_t) is almost the same (77 vs. 76). However, for design OF_1, $N_p = 4$ and $N_t = 55$.

As expected, the lowest total annual is obtained for OF_3. It is 7.05 and 14.53% lower compared to OF_1 and OF_2, respectively. Also, a detailed comparison in Table 4 shows that the optimal values of the all variables for OF_3 (excluding the oil side pressure drop), range between the optimal values obtained for OF_1 and OF_2. From a computational aspect, it is interesting and useful result because the values obtained for OF_1 and OF_2 can be systematically used as lower and upper bounds to solve OF_3. In fact, lower and upper bounds are valuable especially when the mathematical model including the objective function involves non-convex constraints which usually lead to local optimal solutions and/or convergence problems. In other words, it is possible to develop a systematic solution strategy involving a pre-processing phase where optimization problems involving objective functions OF_1 and OF_2 are first solved and both solutions are then used in a second step as bounds to solve the optimization problem involving OF_3. The possibility of developing the mentioned strategy will be further studied in detail in a future work.

Table 2
Numerical values used for model verification.

Validation model	
Tube bundle geometry	
Tube length [L, m]	10.9728
Bundle width [W, m]	3.6
Tube OD	25.4
Tube ID	20.574
Transverse pitch [P_t, mm]	63.5
Longitudinal pitch [P_l, mm]	54.991
Number of passes [N_p]	4
Number of row [N_r]	4
Tubecount rows [N_t]	56
Fins geometry	
Fins/length [N_f, fin/m]	393.7
Height [H_f, mm]	15.875
Thickness [L_f, mm]	0.3302
Fan Geometry	
Number of bays	2
Fan diameter [D_{fan}, m]	3.2

Table 3
Comparison of results (model verification).

	Serth 2007 [14]	XACE simulator	GDP model (Design_1)
Air side pressure drop [ΔP_{fan}, Pa]	89.67	79.67	78.96405
Oil side pressure drop [ΔP_{oil}, kPa]	105.49044	112.523	112.4549
Outside film coefficient [h_o, W/(m^2 h)]	43.84	44.33	44.365
Tubeside film coefficient [h_i, W/(m^2 h)]	2383.29	2780.07	2779.698
Actual U [U_D, W/(m^2 h)]	25.25	26.473	26.296
Required U [U_{req}, W/(m^2 h)]	23.27	23.429	22.839
Area [A, m^2]	4180.37	4143.63	4211.94
Fan power consumption [W_{motor}, kW]	11.56	10.61	10.662
Total annual cost [TAC, $/yr]	98494.23	97059.54	97623.11
CPU time (s)	–	–	0.655
Number of iterations	–	–	121
Explored nodes	–	–	7

4.2.1. Sub-optimal designs

Finally, the mathematical model is solved for two different sub-optimal designs which differ from the optimal configuration design discussed in the previous section. Despite that both designs were obtained for the same objective function (total annual cost) and the input data shown in Table 1 they significantly differ from the optimal design obtained for OF_3 and reported in column 3 of Table 4.

In the first sub-optimal design, hereafter referred as SUB_OP1, the dimensions (tube length and bundle width) of the ACHE were limited by introducing the following inequality constraints:

$$L = 10.97 \text{ m}$$

$$W = 3.60 \text{ m}$$

where the values of 10.97 and 3.6 m correspond to the case study discussed for the model verification (Design_1) which are different to the optimal values reported in the previous section (OF_1, OF_2 and OF_3). In this case, the configuration of the ACHE was considered as optimization variable and consequently it was obtained as a result of model. In contrast to this, in the second sub-optimal design, hereafter referred as SUB_OP2, the model is solved for a fixed type of finned, which is different to that obtained in SUB_OP1. To do this, the binary variable that denotes the type of finned tube II (c_2) is set to one. The study of SUB_OP2 allows to investigate the influence of the type of fin on the optimal cost solution.

The optimal solution obtained corresponding for each sub-optimal design is listed in Table 5.

As shown, the total costs for SUB_OP1 and SUB_OP2 are 6.50 and 7.76% higher compared to the optimal design OF_3 (forth column in Table 4).

By comparing the designs SUB_OP1 and OF_3, it is possible to conclude that for the same transferred heat (4023.073 kW), the

Table 4
Optimal solutions obtained for three optimization criteria.

	Minimizing the heat exchanger area (OF_1)	Minimizing the fan power consumption (OF_2)	Minimizing the TAC (OF_3)
Tube bundle geometry			
Tube length [L, m]	11.292	14.728	13.261
Bundle width [W, m]	3.173	4.889	4.388
Transverse pitch [P_t, mm]	57.15	63.5	57.15
Longitudinal pitch [P_l, mm]	49.5	55	49.5
Number of passes [N_p]	4	3	3
Number of row [N_r]	4	3	3
Number of tubes per rows [N_t]	55	77	76
Fin geometry			
Fins/length [N_f, fin/m]	354.33	393.7	354.33
Height [H_f, mm]	12.7	15.875	12.7
Thickness [L_f, mm]	0.36	0.3	0.36
Fin outside diameter [D_f, mm]	50.8	57.15	50.8
Fan geometry			
Fan diameter [D_{fan}, m]	3.02	4.737	4.235
Process variables			
Air side pressure drop [ΔP_{air}, Pa]	99.92	22.33	34.507
Oil side pressure drop [ΔP_{oil}, kPa]	118.77	63.62	59.78
Outside film coefficient [h_0,W/(m^2 h)]	54.802	34.892	44.22
Tubeside film coefficient [h_i, W/(m^2 h)]	2819.55	2161.4	2183.85
Actual U [U_D, W/(m^2 h)]	34.838	21.338	28.623
Required U [U_{req}, W/(m^2 h)]	33.179	16.509	27.26
Area [A, m^2]	2899.263	5826.8	3528.76
Reynolds number (gas side)	9540	4349	5878
Gas velocity (inlet condition) [m/s]	5.162	2.353	3.181
Oil velocity [m/s]	2.154	1.538	1.559
Fan power consumption [W_{motor}, kW]	13.474	2.771	4.295
Total investment [$/yr]	76750.862	94877.142	79242.1764
Total operating cost [$/yr]	12934.869	2660.018	4123.193
Total annual cost [TAC, $/yr]	89685.731	97537.160	83365.369
CPU time (s)	0.842	1.404	0.624
Number of iterations	574	451	193
Explored nodes	34	25	7

heat transfer area for SUB_OP1 is much smaller than that required by OF_3 (2938.636 m^2 vs. 3528.76 m^2) as a consequence of a higher heat transfer coefficient (U_{req}) required in SUB_OP1 compared to OF_3. However, a higher required heat transfer coefficient leads to increase the velocity and pressure drops in both sides of the ACHE resulting in higher power consumed by fans. Certainly, the total investment cost for SUB_OP1 is about 2.96% lower than that involved by OF_3 and the cost of electricity required by fans is 188.3% higher than OF_3 which result in a higher total cost (88779.555 vs. 83365.369 $/yr).

Also, it is possible to observe that the same optimal fins geometry is obtained for both SUB_OP1 and OF_3 but the optimal number of passes and number of tube rows for SUB_OP1 and OF_3 are, respectively, 4 and 3 which lead to reduce the fan diameter in about 1 m (3.2 vs. 4.235 m).

Regardless to the suboptimal design SUB_OP2 its total cost increases in about 7.76% in comparison to the optimal design (OF_3) as a consequence of the increasing of both the heat transfer area and the electricity consumption by the fans. The increasing of the heat transfer area affects the total cost more significantly than the increasing of the electricity consumption.

In addition, the tube length and bundle width do not vary significantly in contrast to what is observed for the transverse and longitudinal tube pitches, number of passes and number of tubes per rows. In addition, the same optimal number of passes and number of rows are obtained for SUB_OP2 and OF_3 (3 each).

In OF_3, the fin geometry is an optimization variable obtaining the fin geometry that correspond to c_1 while in SUB_OP2 the fin geometry is that correspond to c_2 and is fixed for comparison purposes.

Finally, the comparison results between both sub-optimal designs show that despite the total costs for SUB_OP1 and SUB_OP2 are similar, both designs differ significantly. The dimensions corresponding to design SUB_OP1 and consequently the heat transfer area are significantly smaller than that obtained for SUB_OP2 (30.00%) but the electricity consumption required by the fans is considerably higher (151.00%) as a consequence of the increasing of the pressure drop in the fans (ΔP_{fan}). Certainly, in SUB_OP1, the air and oil velocities increase to enhance the corresponding heat transfer coefficients which results in higher pressure drops. Finally, the pressure drop in the oil side is significantly higher than in the air side.

4.3. Study of the influence of the initialization variables on the model convergence. Performance of different NLP solvers

As mentioned earlier, the proposed model SBB is used to solve the MINLP model. It is based on a combination of the standard B&B (Branch and Bound) method and some of the standard NLP solvers already supported by GAMS (MINOS, CONOPT, among others). MINOS is based on a reduced-gradient algorithm (Wolfe 1962 [20]) combined with a quasi-Newton algorithm (GAMS/MINOS [21]) whereas CONOPT solver is based on the generalized reduced gradient (GRG) algorithm suggested by Abadie and Carpentier 1969 [22]. Details on how both algorithms work can be found in Refs. [19,21,23].

In several optimization models the initialization of variables plays an important role in the model convergence, especially if the model size is large and involves many non linear constraints. Despite of the fact that the proposed model involves 153 variables (1 integer variables, 18 binary variables and 135 continuous variables) and 168 constraints (equality and inequality constraints), it is interesting to investigate the influence of the initialization values

Table 5
Sub-optimal designs.

	Minimizing TAC subject to space limitation	Minimizing TAC using the type of finned tube II [C_2 = True, $c_2 = 1$]
Tube bundle geometry		
Tube length [L, m]	10.85	12.56
Bundle width [W, m]	3.36	4.18
Transverse pitch [P_t, mm]	57.15	63.5
Longitudinal pitch [P_l, mm]	49.5	55
Number of passes [N_p]	4	3
Number of row [N_r]	4	3
Tubecount per rows [N_t]	58	65
Fin geometry		
Fins/length [N_f, fin/m]	354.33	393.7
Height [H_f, mm]	12.72	15.87
Thickness [L_f, mm]	0.36	0.36
Fin outside diameter [D_f, mm]	50.81	57.15
Fan geometry		
Fan diameter [D_{fan}, m]	3.2	4.03
Process variables		
Air side pressure drop [ΔP_{fan}, Pa]	97.66	38.65
Oil side pressure drop [ΔP_{oil}, kPa]	104.87	74.159
Outside film coefficient [h_0, W/(m^2 h)]	54.458	40.167
Tubeside film coefficient [h_i, W/(m^2 h)]	2703.698	2470.954
Actual U [U_D, W/(m^2 h)]	34.371	24.047
Required U [U_{req}, W/(m^{2}hr)]	32.735	22.902
Heat transfer area [A, m^2]	2938.636	4200.342
Reynolds number (gas side)	9412	6155
Gas velocity (inlet condition) [m/s]	5.093	3.331
Oil velocity [v_{oil}, m/s]	2.042	1.822
Fan power consumption [W_{motor}, kW]	12.384	4.924
Investment cost [$/yr]	76890.881	85107.532
Operating cost [$/yr]	11888.674	4726.607
Annual Cost [TAC, $/yr]	88779.555	89834.139
CPU time (s)	1.107	1.389
Number of iterations	168	606
Explored nodes	7	34

and the performance of CONOPT and MINOS solvers on the model convergence.

The performance of both NLP solvers was evaluated in terms of different initialization procedures. One of the strategies was to start the optimization run from the configuration related to the type of finned tube I for which it was necessary to initialize the corresponding variables properly ($c_1 = 1$ and $c_2 = 0$). Then, an opposite initialization was also tested. That is, the model was initialized from the configuration related to the type of finned tube II ($c_1 = 0$ and $c_2 = 1$). In all optimization runs and for both initialization ways, the MINLP solver (SBB) found the same optimal solutions independently of the NLP solver used (CONOPT or MINOS). Finally, random values were also used as initialization. The obtained results reveal that when CONOPT is used as NLP solver the model converged for all simulations and optimizations. However, when MINOS is used, the random initialization failed for some of the simulation and optimization runs. Then, it is possible to conclude that the convergence of the model does not depend on the initialization values when CONOPT is used as NLP solver.

5. Conclusions

In this paper, a disjunctive mathematical model for the optimal design of air cooled heat exchangers was presented. The resulting GDP (generalized disjunctive programming) model involves disjunctions, Boolean variables and logical propositions to model discrete decisions which are then reformulated as a MINLP (mixed integer non linear programming). The resulting model was implemented in GAMS and solved using a branch and bound method (SBB). For a given the heat load to be removed from a hot stream (oil), the model predicts the optimal selection of the type of the flow regime, the type of the finned tube, number of tube rows, number of tube per row, number of passes, fins per unit length and the mean fin thickness. In addition, the optimal dimensions (fan diameter, bundle width, tube length), heat transfer area, pressure drops and velocities in both sides of the ACHE are also obtained as a result.

One of the optimization problems studied in this paper consisted of determining the overall equipment configuration in order to minimize the total annual cost (OF_3) which includes investment (fan and heat transfer area) and operating costs (fan power consumption). For the same design specification, the model was also solved for two other objective functions: a) minimization of the heat transfer area (OF_1) and b) minimization of the fan power consumption (OF_2). In addition, sub-optimal designs (SUB_OP1 and SUB_OP2) were also obtained and compared. Optimized results for each design are summarized and compared in Tables 4 and 5. As expected, the optimal configuration and operating conditions depends strongly on the objective function used for the optimization.

The obtained results clearly show the importance of developing mathematical models that allow to optimize both discrete and continuous decisions simultaneously. A significant reduction on the total annual cost is reached when all the trade offs existing among discrete and continuous decisions were optimized simultaneously. For instance, the optimal cost design (OF_3) is almost 7.00% lower than those design configurations proposed in an arbitrary way and different from the optimal design.

The obtained results also confirm that the optimal values obtained for OF_3 range between the optimal values obtained for OF_1 and OF_2. This may be efficiently used as a guideline to develop a systematic solution strategy, with general applications. The strategy may be separated in two phases. In the first phase, the problems involving OF_1 and OF_2 may be solved and then, in the second phase, they may be used as lower and upper bounds to solve OF_3. In addition, an initial feasible solution to solve OF_3 is also obtained from the first phase of the solution strategy. This is important because more complete mathematical models including detailed cost models which usually involve highly non-linear and non-convex constraints may be easily solved. This strategy will be further developed in detail.

Acknowledgments

Financial supports obtained from the Consejo Nacional de Investigaciones Científicas y Técnicas (CONICET), the Agencia Nacional para la Promoción de la Ciencia y la Tecnología (ANPCyT), the Universidad Tecnológica Nacional Facultad Regional Rosario (UTN-FRRo)-Argentina are greatly acknowledged.

References

[1] González MT, Petracci NC, Urbicain MJ. Air-cooled heat exchanger design using successive quadratic programming (SQP). Heat Transf Eng 2001;22(3):11–6.
[2] Evenko VI . Optimizing air-cooled heat exchanger tube bundle parameters. Chem Pet Eng 2002;38(1–2):41–7.
[3] Doodman AR, Fesanghary M, Hosseini R. A robust stochastic approach for design optimization of air cooled heat exchangers. Appl Energy 2009;86:1240–5.
[4] Salimpour MR, Bahrami Z. Thermodynamic analysis and optimization of air-cooled heat exchangers. Heat Mass Transf 2011;47:35–44.
[5] Pieve M, Salvadori G. Performance of an air-cooled steam condenser for a waste-to-energy plant over its whole operating range. Energy Convers Manag 2011;52(4):1908–13.
[6] Vecchietti A, Grossmann I. Logmip: a disjunctive 0–1 non-linear optimizer for process system models. Comput Chem Eng 1999;23(4–5):555–65.

[7] Van den Heever S, Grossmann I. Disjunctive multiperiod optimization methods for design and planning of chemical process systems. Comput Chem Eng 1999;23(8):1075–95.
[8] Oldenburg J, Marquardt W. Disjunctive modeling for optimal control of hybrid systems. Comput Chem Eng 2008;32(10):2346–64.
[9] You F, Castro P, Grossmann I. Dinkelbach's algorithm as an efficient method for solving a class of MINLP models for large-scale cyclic scheduling problems. Comput Chem Eng 2009;33:1879–89.
[10] Marchetti PA, Méndez CA, Cerdá J. MILP monolithic formulations for lot-sizing and scheduling of single-stage batch facilities. Ind Eng Chem Res 2010;49. ISSN: 0888-5885:6482–98.
[11] Cafaro DC, Cerdá J. A rigorous mathematical formulation for the scheduling of tree-structure pipeline networks. Ind Eng Chem Res 2011;50. ISSN: 0888-5885:5064–85.
[12] Ponce-Ortega J, Pham V, El-Halwagi M, El-Baz A. A disjunctive programming formulation for the optimal design of biorefinery configurations. Ind Eng Chem Res 2012;51(8):3381–400.
[13] García-Ayala G, Ríos-Mercado R, Chacón-Mondragó O. A disjunctive programming model and a rolling horizon algorithm for optimal multiperiod capacity expansion in a multiproduct batch plant. Comput Chem Eng 2012;46:29–38.
[14] Serth RW. Process heat transfer: principles, applications and rules of thumb. 1st ed. Oxford: Elsevier; 2007.
[15] Kern DQ. Process heat transfer. India: McGraw-Hill Education; 1950.
[16] Mills AF. Basic heat and mass transfer. 2nd ed. Prentice Hall; 1999.
[17] Henao Uribe CA. Simulación y evaluación de procesos químicos. Universidad Pontificia Bolivariana; 2005.
[18] Ludwig EE. Applied process design for chemical and petrochemical plants, vol. 3. Gulf Professional Publishing; 2001.
[19] Brooke A, Kendrick D, Meeraus A. GAMS: release 2.25: a user's guide. Scientific Press; 1992.
[20] Wolfe P. The reduced gradient method. Unpublished manuscript. RAND Corporation; 1962.
[21] GAMS/MINOS. http://www.gams.com/dd/docs/solvers/minos.pdf.
[22] Abadie J, Carpentier J. Generalization of the Wolfe reduced gradient method to the case of nonlinear constraints. In: Fletcher R, editor. Optimization. New York: Academic Press; 1969. p. 37–47.
[23] Drud AS. CONOPT: a system for large scale nonlinear optimization. Reference Manual for CONOPT Subroutine Library. Bagsvaerd, Denmark: ARKI Consulting and Development A/S; 199669 p., http://www.gams.com/dd/docs/solvers/conopt.pdf.